Path Planning and Tracking for Vehicle Collision Avoidance Based on Model Predictive Control With Multiconstraints

Article *in* IEEE Transactions on Vehicular Technology · January 2016

DOI: 10.1109/TVT.2016.2555853

CITATIONS
87

READS
806

4 authors, including:

W.W. Melek
University of Waterloo
107 PUBLICATIONS **1,476** CITATIONS

SEE PROFILE

Yanjun Huang
University of Waterloo
66 PUBLICATIONS **469** CITATIONS

SEE PROFILE

Path Planning and Tracking for Vehicle Collision Avoidance based on Model Predictive Control with Multi-constraints

Jie Ji, Amir Khajepour, William Melek, and Yan-Jun Huang

***Abstract*—A path planning and tracking framework is presented in order to maintain a collision free path for autonomous vehicles. For path planning approaches, a 3D virtual dangerous potential field is constructed as a superposition of trigonometric functions of the road and the exponential function of obstacles, which can generate a desired trajectory for collision avoidance when a vehicle collision with obstacles is likely to happen. Next, in order to track the planned trajectory for collision avoidance maneuvers, the path tracking controller formulates the tracking task as a Multi-constrained Model Predictive Control (MMPC) problem, and calculated the front steering angle to prevent the vehicle from colliding with a moving obstacle vehicle. Simulink and CarSim simulations are conducted in the case where moving obstacles exist. The simulation results show that the proposed path planning approach is effective for many driving scenarios and the MMPC-based path-tracking controller provides dynamic tracking performance and maintains good maneuverability.**

***Index Terms*—Autonomous vehicle, collision avoidance, model predictive control, multi-constraints, path planning, path tracking**

I. Introduction

OWING to the rapid increase in traffic density, vehicle safety has become a crucial factor in modern intelligent transportation systems. While passive safety systems, in combination with ever-increasing active safety systems in motor vehicles have been developed to avoid vehicle crashes and minimize the impact of accidents [1], the need for further reduction in traffic accident incidences using modern control and sensing technologies remains of great interest. In recent years, autonomous vehicles have attracted strong attention from the automotive industry due to their potential applications in collision avoidance. However, fully autonomous driving for the objective of having 'zero accidents on the road' remains a complex task. Further work, such as planning the path upon detecting obstacles, and controlling the actuators so that the vehicle follows the planned path, is often required before the collision avoidance system is road-ready.

Although there has been substantial research on path planning and tracking in collision avoidance systems for unmanned aerial vehicles (UAV) and other robots [2]-[5], It is not easy to apply these approaches directly to vehicle collision scenarios, since the vehicle can only move at the limits of its stability and handling capability in a constrained environment. Furthermore, to solve the collision avoidance problems on the road, it is also necessary to consider other moving vehicles that have these own motion properties.

The path planning for a vehicle collision avoidance system is to generate a collision-free trajectory which takes into consideration geometric characteristics of obstacles and the kinematic constraints of the autonomous vehicle [6]. Early works on path planning for autonomous vehicles date back to the 1980s and were primarily focused on computing a time-optimal and collision-free trajectory going from a given point to another [7] and [8]. Since then, many different computational methods and various successful implementations have been reported in research literature.

The common path planning methods include A* heuristic search, visibility graph method, generalized Voronoi diagram and artificial potential field [6]. The artificial potential field (APF) method was inspired by classical mechanics; it formulates a relationship between the motion of the autonomous vehicle and the sum of the applied forces [9]. This method has been used to generate repulsive potential fields to obstacles and attractive potential fields to the goal, which enables the vehicle to avoid collisions with obstacle boundaries while proceeding towards its goal. The APF-based method is very different from previously mentioned approaches, which have all future path information known after the planner's execution and before the vehicle's motion [10]. However, traditional APF-based path planning approaches possess an inherent problem, which is the formation of local minimum that

Manuscript received February 17, 2015; revised September 14, 2015; accepted March 22, 2016. Date of publication May **, 2016; date of current version April 15, 2016. The work of J. Ji was supported in part by the National Natural Science Foundation of China under Grant 61304189, by the Fundamental Research Funds for the Central Universities under Grant XDJK2015B028, and by the Basic and Cutting-edge Research Projects in Chongqing under Grant cstc2015jcyjA60007. The work of A. Khajepour, W. Melek and Y-J. Huang was supported by the Natural Sciences and Engineering Research Council of Canada. The review of this paper was coordinated by Prof. J-M. Wang.

J. Ji is with the College of Engineering and Technology, Southwest University, Chongqing, 400715, China (e-mail: jijiess@163.com).

A. Khajepour, W. Melek and Y-J. Huang are with the Department of Mechanical and Mechatronics Engineering, University of Waterloo, Ontario, N2L3G1, Canada (e-mail: a.khajepour@uwaterloo.ca; william.melek@uwaterloo.ca; y269huan@uwaterloo.ca).

Color versions of one or more of the figures in this paper are available online at http://ieeexplore.ieee.org.

Digital Object Identifier 10.1109/TVT.2015.*******

may prevent the vehicle from arriving at the target [11].

In this work, a new 3D potential field that can generate collision free trajectory for autonomous vehicle is developed based on the boundary conditions of the road and the vehicle's kinematic model. Collision avoidance conditions are established and the algorithm can be updated in real time to obtain a collision-free trajectory in a complex workspace involving static and dynamic obstacles.

A successful collision avoidance maneuver does not end with just path planning but extends to path tracking that aims to ensure that the vehicle will follow a planned trajectory as close as possible [12].

The commonly used methods for path tracking of autonomous vehicle include fuzzy logic [13], sliding-mode control [14], and robust control [15]. However, many of these control applications assumed that the calculated inputs would never reach the saturation limits of the actuators yet, in practice, this is not true. Moreover, vehicles are made up of mechanical and electrical parts, which are also subjected to physical constraints. Thus, nonlinear characteristics of vehicles and their interactions with road must be considered. The model predictive control (MPC) is an attractive method to tackle this problem [16]. Because of its capability to systematically handle input constraints, and admissible states, model predictive control with multi-constraints is adopted to track the planned trajectory for collision avoidance in this work.

Here, the path tracking problem is formulated as a MPC problem with multi-constraints. At each sampling time instant, a future input sequence of front steering angle for collision avoidance can be calculated in a defined horizon. This is accomplished by solving a finite-time optimal control problem, considering a set of constraints in both the control actions and the plant outputs [16]. An additional feature of a MPC-based approach for collision avoidance is that it continuously optimizes the performance index by receiving information about vehicle position, heading angle and obstacles as the vehicle moves [17].

This paper presents a path planning approach based on the theory of virtual potential field and a path tracking framework using multi-constrained model predictive control for autonomous vehicles, which seeks to minimize the incidence for collision on roads. By receiving information about vehicle position, road parameters, and obstacles surrounding the vehicle, this framework provides a vehicle trajectory for a collision avoidance system based on a 3D virtual dangerous potential field, which seeks to minimize risk to the vehicle through evasive maneuvering. A MMPC-based path-tracking system, considering the geometric constraints of road and dynamic constraints of the vehicle, calculates the steering wheel angle in order to track the planned trajectory and to avoid obstacles. Simulations in different scenarios show the effectiveness of the proposed approach. In particular, MPC with constraint of the steering angle is compared with the proposed approach in terms of performance and constraint satisfaction.

The remainder of this paper is organized as follows: in the next section, the problem and overall framework of the collision avoidance system are introduced. Section III describes the path-planning algorithm that determines a collision-free trajectory based on the 3D dangerous potential field. Section IV develops the augmented vehicle dynamic model used for path tracking. Section V presents the main contribution of this work and details multi-constrained model predictive control. The effectiveness of the proposed framework is demonstrated through simulations in Section VI. Finally, conclusions are provided in Section VII.

II. Description of Collision Avoidance System

A. Problem description

The majority of traffic accidents on roads are caused by vehicle collision. The objective of any collision avoidance system is to design a vehicle control algorithm to avoid an imminent accident. Longitudinal control (i.e., emergency braking only), and lateral control, (i.e., active steering only), are possible choices of actuation configuration for collision avoidance maneuver [18]. Fig. 1 represents the aforementioned two maneuvers.

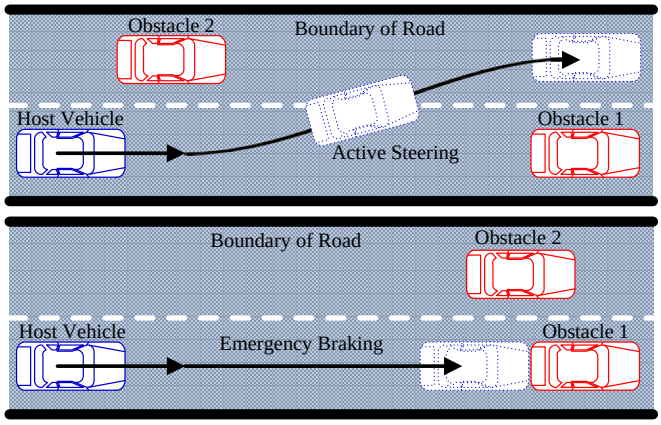

Fig. 1. Problem description of collision avoidance on road.

It is becoming increasingly common for luxury cars to be fitted with Emergency Brake Assist (EBA) or Brake Assist System (BAS). However, longitudinal collision avoidance controllers are of limited benefit for preventing head-on collisions between road vehicles travelling at high speed or for rear end collisions when there is insufficient separation between the vehicles. In these circumstances, aggressive lateral vehicle maneuvers are more appropriate, as is altering the path of the vehicle to move it out of danger. The maneuvers in this case can be completed in a shorter distance than that required to stop the vehicle. This paper focuses purely on the steering control of an autonomous vehicle to track the planned trajectory and to perform an emergency collision avoidance maneuver.

B. Framework of collision avoidance system

The proposed collision avoidance framework aims to generate a collision-free trajectory at any instance and keeps the vehicle as close as possible to the planned trajectory. The trajectory is updated at the same control cycle to handle any changes in the obstacles locations and speeds. The overall proposed architecture is presented in Fig. 2.

The architecture in Fig. 2 describes the main elements of a collision avoidance system, which is composed of three blocks: the collision free trajectory generator, the path-tracking control system, and the virtual simulation environmental model.

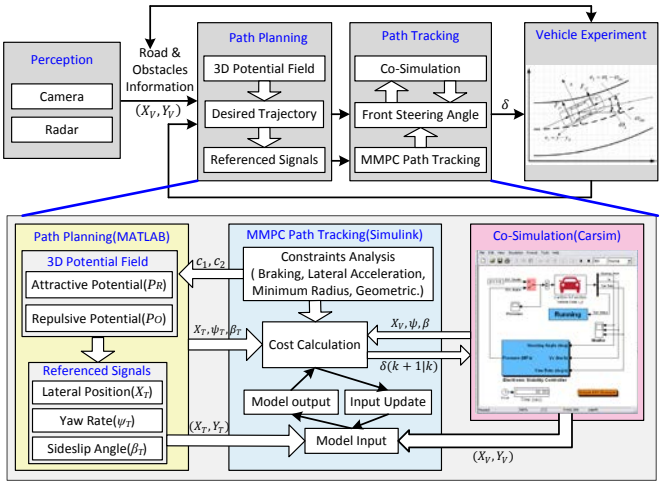

Fig. 2. Overall architecture of collision avoidance system.

The path planning block in this architecture generates a collision free trajectory during runtime. In the case of a vehicle traveling on the road, it can be planned based on occurrence of certain events such as: a stationary obstacle or moving vehicle is detected in the path. Moreover, the referenced signals of lateral position, yaw rate, and sideslip angle of the simplified model are the state variables for MMPC that can be calculated from the planned trajectory in this block.

The path-tracking module is based on a receding horizon control design [19]. The tracking problem is formulated as a constrained optimization problem. The cost function penalizes lateral tracking errors between the predicted position of vehicle and the planned trajectory derived of the 3D potential field. Furthermore, the penalty of the yaw rate tracking errors will play a main role in cost function when the yaw rate error exceeds its threshold. Regarding the vehicle sideslip regulation, the desired sideslip is simply defined via a tolerance band around the sideslip angle (β_{curv}) that also takes account of the sign of the rate of sideslip angle ($\dot{\beta}_{curv}$).

In simulations presented in the paper, the control inputs obtained by the path tracking block are applied to the CarSim vehicle model. CarSim is software which builds full non-linear models of actual vehicles when parameters such as dimensions of the vehicle platform, specifications of the engine and tires, and coefficients of the suspensions are known. The CarSim vehicle model has been validated with experimental results on an actual vehicle [21]. For simplicity, it is assumed that all vehicle variables, brake torques, tire forces and the surface friction coefficient are available to the controller by direct measurements or through estimation algorithm in CarSim

III. Path Planning for Collision Avoidance Using 3D Virtual Dangerous Potential Field

This section focuses on formulating a path planning algorithm for the collision avoidance system based on 3D virtual dangerous potential field. Many researchers have studied path planning for autonomous vehicle and a number of rule-based methods have been proposed, such as virtual desired trajectory [20] and [21] and elastic band theory [22], etc. However, driving is a complex task, and even highway subtleties make the implementation of a rule-based planning algorithm cumbersome. Therefore, utilizing an artificial potential field for local trajectory planning offers an elegant alternative [23]. This method can modify the collision free trajectory in real time. So, potential function approaches have already seen considerable use for path planning of autonomous vehicle [24].

In order to simplify the derivation of the collision-free trajectory using the potential field approach, this paper assumes the following conditions [25], as illustrated in Fig. 1.

☐The road is straight with road boundaries on both sides.

☐Only a single obstacle appears in front of the host vehicle when it is in motion.

☐Regardless of vehicle avoidance action, the obstacle continues moving along the road.

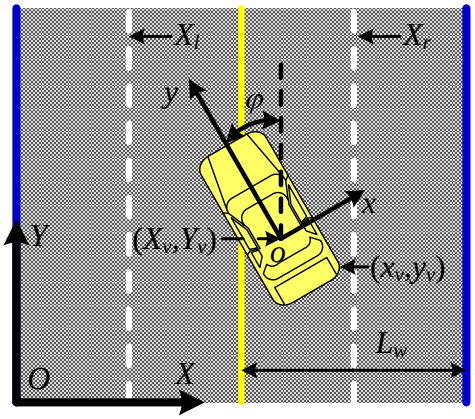

Fig. 3. Fixed earth and vehicle body axis systems.

Two coordinate systems, vehicle body and fixed earth, respectively, are shown in Fig. 3. The vehicle body coordinate system is a right-hand orthogonal axis set (x, o, y) centered on the vehicle's center of mass with y defined positive forwards along the centerline of the vehicle and x defined positive to the right [26]. Since this axis system moves with the vehicle, it is not useful for measuring vehicle position relative to the ground. Therefore, a fixed earth coordinate system (X, O, Y) is defined to be co-located and aligned with the vehicle axis at some point before the start of any maneuver but does not subsequently move or rotate with the vehicle. The coordinates of vehicle's center of mass in fixed earth coordinate system are (X_v, Y_v). The X-axis is along the perpendicular of lane centerline, while Y-axis is in the direction of lane centerline. With the above assumptions, both the road and the vehicle's motion state are described in fixed earth coordinate system. The horizontal angle of rotation between these axis systems is the vehicle heading angle φ, X_l and X_r are the coordinates of centerline of left lane and right lane in X direction of fixed earth coordinate system, L_w denotes the width of each lane.

The proposed universal potential $P_U(X, Y)$ is obtained by

adding the repulsive potential $P_O(X,Y)$ resulting from all obstacles and the attractive potential $P_R(X,Y)$ resulting from the target trajectory, where each fulfills a particular role in the path planning task [27].

In order to present the mathematical function of the potential field, the potential of the road in the absence of obstacles will be presented first. The attractive potential of the road $P_R(X,Y)$, prevents the vehicle from drifting off the highway and guides the vehicle into the center of its lane, but is also small enough to be easily overcome in the case that a lane change is necessary for collision avoidance. The mathematical expression of the potential function expressed in the fixed earth coordinate system is considered as:

$$P_R(X,Y) = A(X)A(Y) + P_A(X,Y) \tag{1}$$

The function has two maximums related to the road boundaries and two minimums related to the centerlines of both lanes. $A(X)$ and $A(Y)$ determine the amplitudes of the potential field along the width and length of road, respectively. $P_A(X,Y)$ denotes an attractive potential driving the autonomous vehicle forwards in the region of universal potential field and leading vehicle towards the centerline of right lane when it has passed the obstacles ahead. A form for the functions $A(X)$, $A(Y)$ and $P_A(X,Y)$ can be considered as:

$$A(X) = \frac{[|sgn(X-X_l)+sgn(X-X_r)|(1-P_m)+2P_m]\left[\cos\left(\frac{2\pi X}{L_W}\right)+1\right]}{4} \tag{2}$$

$$A(Y) = \begin{cases} 0, & |Y-Y_o| \le D_b \\ \frac{|Y-Y_o|-D_b}{D_t-D_b}, & D_b < |Y-Y_o| \le D_t \\ 1, & else \end{cases} \tag{3}$$

$$P_A(X,Y) = \frac{|X-X_r|+|Y-(Y_o+0.5D_s)|}{100} \tag{4}$$

where P_m indicates the amplitude of potential of the middle line of road, Y_o is the position of obstacle in Y direction of the fixed earth axis system, D_b is the shortest braking distance of 'big sedan' model in CarSim, and it can be calculated by equation (8), D_t and D_s denote the scope of the repulsive and universal potential field for collision avoidance in Y direction of fixed earth axis system respectively.

The three-dimensional graphical representation of the function defined in (1) is illustrated in Fig. 4.

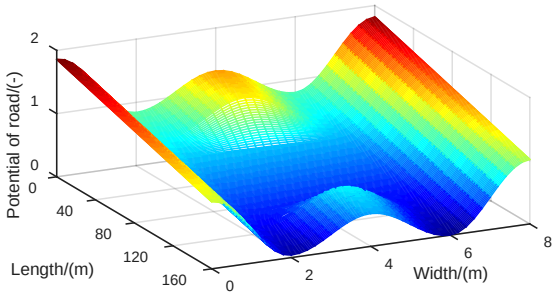

Fig. 4. 3D attractive potential field of the road.

For the potential of an obstacle or leading vehicle, a cost function using the information of the distance and angle to the detected obstacles from the vehicle is used for generating the repulsive potential field. The potential must be shaped to keep the vehicle a safe distance from any obstacle and also encourage lane changing if there is not enough longitudinal space for the host vehicle to avoid the obstacle by braking. The mathematical expression of a potential function for an obstacle or a leading vehicle can be expressed in the fixed earth axis system as:

$$P_O(X,Y) = \frac{\left|e^{-c_1(X-X_O)^2-c_2(Y-Y_O)^2}-P_t\right|}{1-P_t} \tag{5}$$

where X_o is the position of obstacle in X direction of the fixed earth axis system, parameters c_1, c_2, and P_t determine the value and the shape of the potential field associated with the relative speed and distance between the vehicle and the obstacle. P_t denotes the threshold that determines the scope of the repulsive potential field, c_1 is the weight on the lateral distance between vehicle and the obstacle, and c_2 corresponds to the distance between the obstacle and the point from where the collision avoidance maneuver started. c_1, and c_2 can be described as

$$c_1 = \begin{cases} \frac{-ln(P_t)-c_2(Y-Y_0)^2}{\left\{0.5*L_W*\left[sin\left(\frac{Y-Y_0+D_b}{D_b}*\pi-\frac{\pi}{2}\right)+1\right]\right\}^2}, & |Y-Y_o| \le D_b \\ 0, & else \end{cases} \tag{6}$$

$$c_2 = -\frac{ln(P_t)}{D_b^2} = -\frac{64F_m^2 ln(P_t)}{[m(V^2-v^2)+4F_mL_l]^2} \tag{7}$$

$$D_b = \frac{m(V^2-v^2)}{8F_m} + \frac{L_l}{2} \tag{8}$$

where m is the mass of the vehicle, V and v are the longitudinal velocity at the c.g. of vehicle and obstacle, respectively, F_m denotes the maximum braking force of each tire, L_l is the outside diameter of the obstacle.

The three-dimensional graphical representation of the function (5) is illustrated in Fig. 5.

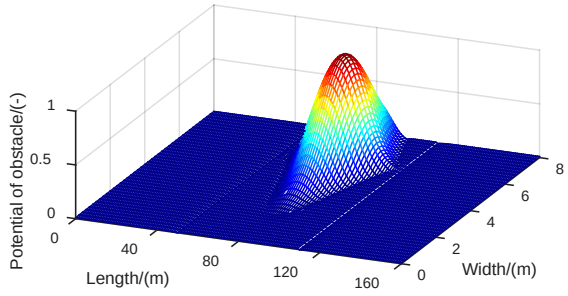

Fig. 5. 3D repulsive potential field of obstacle.

If the attractive potential $P_R(X,Y)$ and repulsive potential $P_O(X,Y)$ are added together, the universal potential function $P_U(X,Y)$ will be:

$$P_U(X,Y) = P_R(X,Y) + P_O(X,Y) \tag{9}$$

Fig. 6, the three-dimensional map of the universal potential field, displays the threats around the autonomous vehicle

on-road at a particular instant in time.

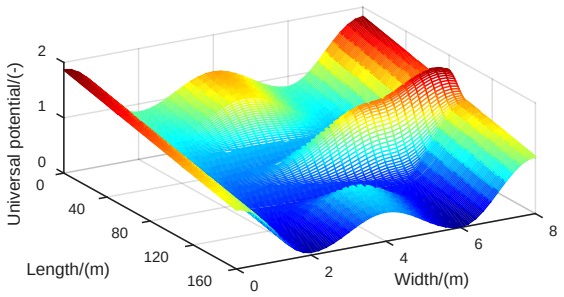

Fig. 6. Universal potential field of road and obstacle.

The negative gradient of universal potential field is defined as induced force which is the steepest descent direction for guiding vehicle to target point. Energy of the collision threats is minimized by following the direction of the induced force.

For the autonomous vehicle is attracted by the road potential and repelled by the obstacle potential, the universal induced force $\overrightarrow{F_U}$ in the sum of an attractive force $\overrightarrow{F_R}$ and a repulsive force $\overrightarrow{F_O}$, whose direction indicates the most promising local direction of motion. The desired motion of the autonomous vehicle from any given position can be determined by the induced force $\overrightarrow{F_U}$, as defined in Fig. 7.

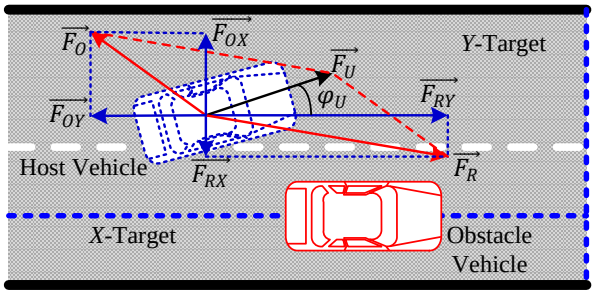

Fig. 7. Direction of reduced force.

As shown in Fig. 7, the universal induced force of vehicle is:

$$\overrightarrow{F_U} = -\nabla P_U(X_v, Y_v) = -\nabla P_R(X_v, Y_v) - \nabla P_O(X_v, Y_v) = \left(\overrightarrow{F_{RX}} + \overrightarrow{F_{RY}}\right) + \left(\overrightarrow{F_{OX}} + \overrightarrow{F_{OY}}\right) \quad (10)$$

Where: $\overrightarrow{F_{RX}}$ and $\overrightarrow{F_{OX}}$ are attractive force and repulsive force in X direction. $\overrightarrow{F_{RY}}$ and $\overrightarrow{F_{OY}}$ are attractive force and repulsive force in Y direction. They can be expressed as:

$$\left[\overrightarrow{F_{RX}} \quad \overrightarrow{F_{RY}} \quad \overrightarrow{F_{OX}} \quad \overrightarrow{F_{OY}}\right] = \left[\frac{-\partial[P_R(X_v,Y_v)]}{\partial X} \quad \frac{-\partial[P_R(X_v,Y_v)]}{\partial Y} \quad \frac{-\partial[P_O(X_v,Y_v)]}{\partial X} \quad \frac{-\partial[P_O(X_v,Y_v)]}{\partial Y}\right] \quad (11)$$

$X_T(k), \beta_T(k)$, and $\psi_T(k)$ are the reference information of planned trajectory, sideslip angle and yaw angle at instance time k, which can be derived by taking small steps in the direction of the universal induced force $\overrightarrow{F_U}$. The two-dimensional contour plot of the resulting universal potential displays the desired collision free trajectory for path tracking of the vehicle, as shown in Fig. 8.

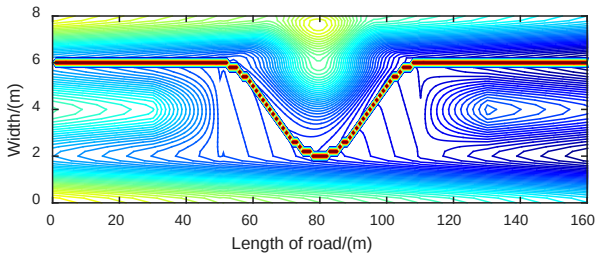

Fig. 8. Contour plot of the potential field and collision free trajectory.

IV. VEHICLE MATHEMATICAL MODEL FOR PATH TRACKING PROBLEM

The path tracking problem is very dependent on the vehicle modeling since it is a requirement for multi-constraints model predictive control law design. The model used in this paper should take into account the kinematic and dynamic aspects of the vehicle [16]. Here, we present an augmented mathematical model of a vehicle used for the development of collision avoidance system. Section *A* develops a vehicle dynamic model along with its lateral and yaw dynamics, and Section *B* introduces a discrete state-space vehicle model used for the development of multi-constrained model predictive controller.

A. Vehicle dynamic model for path tracking

This section describes the vehicle and tire models we used for control design. For the path-tracking problem, the following assumptions are made in the vehicle model: 1) the longitudinal velocity of vehicle is constant, 2) at the front and rear axles, the left and right wheels are lumped in a single wheel, and 3) suspension movements, slip phenomena, and aerodynamic influences are neglected.

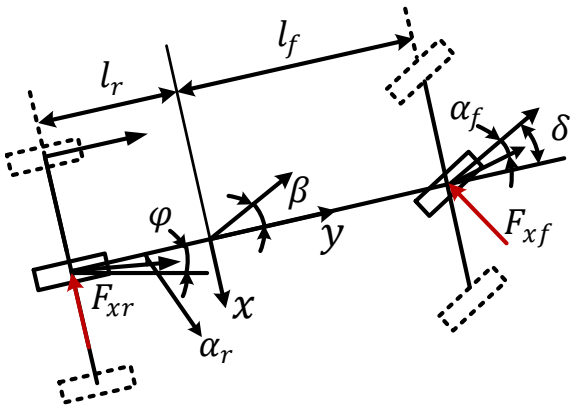

Fig. 9. Vehicle dynamics model used for path tracking.

With these assumptions, the linear dynamic model of a conventional vehicle, as depicted in Fig. 9, is obtained according to Newton's laws. Using the body sideslip angle β and the yaw rate of vehicle body $\dot{\psi}$ as state variables, the vehicle lateral dynamics can then be described by:

$$mV(\dot{\beta} + \dot{\psi}) = F_{xf} + F_{xr} \quad (12)$$

$$I_z\ddot{\psi} = l_f F_{xf} - l_r F_{xr} \quad (13)$$

where I_z is the vehicle moment of inertia about yaw axis, l_f and l_r are the longitudinal distances from the c.g. of vehicle to the front and rear wheels, respectively.

There exist a number of different models for cornering tire forces. For small tire slip angles, the lateral tire forces are approximated as a linear function of tire slip angle. The front and rear tire forces F_{xf}, F_{xr} and tire slip angles α_f, α_r are defined as [28]:

$$F_{xf} = C_f \times \alpha_f = C_f \times \left(\delta - \beta - \frac{l_f \dot{\psi}}{V}\right) \quad (14)$$

$$F_{xr} = C_r \times \alpha_r = C_r \times \left(-\beta + \frac{l_r \dot{\psi}}{V}\right) \quad (15)$$

where δ is the front-wheel steering angle, C_f and C_r represent the linearized cornering stiffness of the front and rear wheels, respectively.

Substituting (14) and (15) into (12) and (13), the equations governing the lateral and yaw dynamics in a vehicle model can be expressed as:

$$\dot{\beta} = \frac{-(C_r + C_f)}{mV}\beta + \left(\frac{C_r l_r - C_f l_f}{mV^2} - 1\right)\dot{\psi} + \frac{C_f}{mV}\delta \quad (16)$$

$$\ddot{\psi} = \frac{C_r l_r - C_f l_f}{I_z}\beta - \frac{C_r l_r^2 + C_f l_f^2}{I_z V}\dot{\psi} + \frac{C_f l_f}{I_z}\delta \quad (17)$$

B. *Discrete linear vehicle model for MPC*

In this section, we derive a discrete state-space vehicle model, for the MMPC optimization process, from the mathematical model obtained in the previous section. In the new vehicle model, the state-space vector is made up of the lateral position of the vehicle c.g. X_v, the vehicle sideslip angle β, yaw angle ψ and the yaw rate $\dot{\psi}$. The input is given by the angle of front wheel δ. With this definition, the state-space vector is obtained as follows:

$$X_c = [X_v \quad \beta \quad \psi \quad \dot{\psi}]^T \quad (18)$$

The state equations can be written based on equations (16) and (17) derived in the previous section as:

$$\dot{X}_c = A_c X_c + B_c \delta \quad (19)$$

$$Y_c = C_c X_c \quad (20)$$

where

$$A_c = \begin{bmatrix} 0 & V & V & 0 \\ 0 & -\frac{C_r + C_f}{mV} & 0 & \frac{C_r l_r - C_f l_f}{mV^2} - 1 \\ 0 & 0 & 0 & 1 \\ 0 & \frac{C_r l_r - C_f l_f}{I_z} & 0 & -\frac{C_r l_r^2 + C_f l_f^2}{I_z V} \end{bmatrix}$$

$$B_c = \begin{bmatrix} 0 \\ \frac{C_f}{mV} \\ 0 \\ \frac{C_f l_f}{I_z} \end{bmatrix}, C_c = \begin{bmatrix} 1 & 0 & 0 & 0 \\ 0 & 1 & 0 & 0 \\ 0 & 0 & 0 & 1 \end{bmatrix} \quad (21)$$

The above vehicle model is a linearized, continuous-time, single-input and multiple-output system. However, the system to be controlled is usually modelled by a discrete state-space model in the MPC literature [29]. Therefore, equations (19) and (20) are transformed into a discrete state-space model to obtain,

$$X_d(k+1) = A_d X_d(k) + B_d u(k) \quad (22)$$

where A_d and B_d are the state and control matrices for discrete state space equation respectively, which can be calculated with the Euler method as:

$$A_d = e^{A_C \Delta T} \quad (23)$$

$$B_d = \int_{k\Delta T}^{(k+1)\Delta T} e^{A_C[(k+1)\Delta T - \tau]} B_C \, d\tau \quad (24)$$

where ΔT is the sampling interval for discrete state-space model.

The lateral displacement, sideslip angle and yaw rate of vehicle are defined as outputs using:

$$Y_d(k) = C_d X_d(k) \quad (25)$$

where

$$Y_d(k) = \begin{bmatrix} X_v \\ \beta \\ \dot{\psi} \end{bmatrix}, C_d = C_c = \begin{bmatrix} 1 & 0 & 0 & 0 \\ 0 & 1 & 0 & 0 \\ 0 & 0 & 0 & 1 \end{bmatrix} \quad (26)$$

In path tracking using MMPC, it is common to formulate the constrained control problem as a real-time optimization problem subject to hard constraints on plant variables and soft constraints on outputs. The discrete state-space model (22) and (25) are augmented as uniform model with integrators [29].

Let us denote the difference of the state variables and the control variable by

$$\Delta X_d(k+1) = X_d(k+1) - X_d(k) \quad (27)$$

$$\Delta X_d(k) = X_d(k) - X_d(k-1) \quad (28)$$

$$\Delta u(k) = u(k) - u(k-1) \quad (29)$$

Substituting equations (27) to (29) into equations (22) and (25), transforms the latter two equations into a discrete state-space model with the increments of the variables $X_d(k)$ and $u(k)$ as

$$\Delta X_d(k+1) = A_d \Delta X_d(k) + B_d \Delta u(k) \quad (30)$$

$$Y_d(k+1) - Y_d(k) = C_d A_d \Delta X_d(k) + C_d B_d \Delta u(k) \quad (31)$$

Note that the input to the state-space model and the output equations is $\Delta u(k)$. In order to connect $\Delta X_d(k)$ to the outputs $Y(k)$. A new state variable vector is chosen as:

$$X_a(k) = \begin{bmatrix} \Delta X_d(k) \\ Y_d(k) \end{bmatrix} \quad (32)$$

Combining equation (32) with equations (30) and (31) yields the following state-space model:

$$X_a(k+1) = A_a X_a(k) + B_a \Delta u(k) \quad (33)$$

$$Y_a(k) = C_a X_a(k) \quad (34)$$

where, the triplet (A_a, B_a, C_a) are called the augmented model, which can be described as follow.

$$A_a = \begin{bmatrix} A_d & O_a^T \\ C_d A_d & I_a \end{bmatrix},\ B_a = \begin{bmatrix} B_d \\ C_d B_d \end{bmatrix},\ C_a = [O_a \quad I_a],$$
$$O_a = \begin{bmatrix} 0 & 0 & 0 & 0 \\ 0 & 0 & 0 & 0 \\ 0 & 0 & 0 & 0 \end{bmatrix},\quad I_a = \begin{bmatrix} 1 & 0 & 0 \\ 0 & 1 & 0 \\ 0 & 0 & 1 \end{bmatrix} \quad (35)$$

V. Design of Multi-Constrained Model Predictive Controller

The path tracking task can be posed as a predictive control problem with the constraints derived from vehicle dynamics and kinematics. The analysis presented in this section is based on [29], but adapted to suit the vehicle collision avoidance application.

A. Prediction of state and output variables

An important step in the design of a model predictive controller for path tracking is to predict the future behavior of the vehicle at each time step. This future prediction determines the control inputs within a specified prediction horizon and, on the basis of these future states, a performance index is minimized to compute the optimal control inputs [12].

Here, we assume that the current time is k, $k > 0$, the prediction horizon is $N_p = 10$ as the length of the optimization window and the control horizon is $N_c = 5$. The state variable vector $X_a(k)$ provides the current plant information, which is available through measurement.

With given information $X_a(k)$, the future state variables can be predicted for N_p steps ahead:

$$X_a(k+1), \cdots, X_a(k+m), \cdots, X_a(k+N_P) \quad (36)$$

where $X_a(k+m)$ is the predicted state variable at $k+m$ with given current plant information $X_a(k)$.

We denote by ΔU_m the sequence of future input increments computed at time k for the current observed states.

$$\Delta U_m = [\Delta u(k), \cdots, \Delta u(k+m), \cdots, \Delta u(k+N_c-1)]^T \quad (37)$$

Using the set of future control parameters ΔU_m and the state-space model (A_a, B_a, C_a), The state variables of the vehicle are calculated sequentially by continuing iteration of equation (33):

$$X_a(k+1) = A_a X_a(k) + B_a \Delta u(k)$$
$$X_a(k+2) = A_a^2 X_a(k) + A_a B_a \Delta u(k) + B_a \Delta u(k+1)$$
$$\vdots$$
$$X_a(k+N_c) = A_a^{N_c} X_a(k) + A_a^{N_c-1} B_a \Delta u(k) + \cdots + B_a \Delta u(k+N_C-1) \quad (38)$$
$$\vdots$$
$$X_a(k+N_P) = A_a^{N_P} X_a(k) + A_a^{N_P-1} B_a \Delta u(k) + \cdots + A_a^{N_P-N_C} B_a \Delta u(k+N_C-1)$$

By using successive substitution, it is assumed that the control input varies for only the N_c time steps (the control horizon) and then is held constant up to the preview horizon [30, 31].

We then define the state vector and predicted outputs for the predictive state-space model as:

$$X_m(k) = X_a(k) =$$
$$[\Delta X_v(k)\ \ \Delta\beta(k)\ \ \Delta\psi(k)\ \ \Delta\dot{\psi}(k)\ \ X_v(k)\ \ \beta(k)\ \ \dot{\psi}(k)]^T \quad (39)$$

$$Y_m(k) = [Y_a(k+1) \quad \cdots \quad Y_a(k+N_p)]^T \quad (40)$$

In this situation, it is straightforward to derive the prediction model of performance outputs over the prediction horizon N_P in a compact matrix form as:

$$Y_m(k) = F_m X_m(k) + G_m \Delta U_m \quad (41)$$

Where

$$F_m = [C_a A_a \ \ C_a A_a^2 \ \ \cdots \ \ C_a A_a^{N_C} \ \ \cdots \ \ C_a A_a^{N_P}]^T_{3N_P \times 7} \quad (42)$$
$$G_m = \begin{bmatrix} C_a B_a & 0 & \cdots & 0 \\ C_a A_a B_a & C_a B_a & \cdots & 0 \\ \vdots & \vdots & \cdots & 0 \\ C_a A_a^{N_C-1} B_a & C_a A_a^{N_C-2} B_a & \cdots & C_a B_a \\ \vdots & \vdots & \ddots & \vdots \\ C_a A_a^{N_P-1} B_a & C_a A_a^{N_P-2} B_a & \cdots & C_a A_a^{N_P-N_C} B_a \end{bmatrix}_{3N_P \times N_C}$$

B. Development of cost function with vehicle dynamics

As described in section 3, the reference location information of planned trajectory $P_r(k)$, sideslip angle $\beta_r(k)$ and yaw rate $\dot{\psi}_r(k)$ at time k are chosen as the given set-point information for MMPC, which are calculated by the universal potential field of road and obstacle within the prediction horizon N_P. The reference signals are described as follows

$$[P_r(k) \quad \beta_r(k) \quad \psi_r(k)] = \begin{bmatrix} X_T(k+1) & \beta_T(k+1) & \psi_T(k+1) \\ X_T(k+2) & \beta_T(k+2) & \psi_T(k+2) \\ \cdots & \cdots & \cdots \\ X_T(k+N_p) & \beta_T(k+N_p) & \psi_T(k+N_p) \end{bmatrix} \quad (43)$$

The objective of MMPC is to bring the predicted outputs $P_v(k)$, $\beta_v(k)$ and $\dot{\psi}_v(k)$ as close as possible to the set-point signals. We define the cost function J_E that reflects the control objective as

$$J_E = [P_r(k) - P_v(k)]^T [P_r(k) - P_v(k)] + [\beta_r(k) - \beta_v(k)]^T [\beta_r(k) - \beta_v(k)] + \left[\dot{\psi}_r(k) - \dot{\psi}_v(k)\right]^T \left[\dot{\psi}_r(k) - \dot{\psi}_v(k)\right] + \Delta U_m^T \bar{R} \Delta U_m \quad (44)$$

where, as in MMPC notation, $P_v(k)$, $\beta_v(k)$ and $\dot{\psi}_v(k)$ are the predicted sequence of lateral position, sideslip angle and yaw rate of vehicle in fixed earth coordinate system, which can be calculated for N_P time steps at time k using equation (34), and ΔU_m is the predicted optimization vector. $\bar{R} = r_w I_{N_C \times N_C} (r_w > 0)$ denotes the cost function matrix associated with the future values of the steer input.

Consider the autonomous vehicle traveling with constant longitudinal velocity V on the planned trajectory, and assume that the curvature of the planned trajectory is C_T at instant time k [28]. The reference sideslip angle of the vehicle is automatically determined by

$$\beta_{curv} = C_T \left(L_r - \frac{L_f m V^2}{2 C_r L} \right) \quad (45)$$

$$C_T = \left| \frac{d^2 X_T}{dY_T^2} \right| \Big/ \left[1 + \left(\frac{dX_T}{dY_T} \right)^2 \right]^{\frac{3}{2}} \quad (46)$$

where $L = L_f + L_r$ is used to denote the wheelbase of the vehicle, X_T, Y_T are the coordinates of the planned trajectory in fixed earth coordinate system, which are derived from the universal potential field.

Following [32] and [33], we require β_{curv} to be limited in the interval $[-\beta_{max}, \beta_{max}]$
where

$$\beta_{max} = \begin{cases} 2\frac{k_1 - k_2}{V_r^3} V^3 - 3\frac{k_1 - k_2}{V_r^2} V^2 + k_1, & if\ V < V_r \\ k_2, & if\ V \geq V_r \end{cases} \quad (47)$$

and V_r is the characteristic speed. Reasonable values for parameters k_1 and k_2 are π/18 and π/60 respectively [32].

When $|\beta(k)| > |\beta_{max}|$ a regulation level $\beta_{ref} = \beta_{max}$ ($\beta_{ref} = -\beta_{max}$) is activated. Thus, we define the reference signal of sideslip angle as

$$\beta_r(k) = \begin{cases} \beta_{max}, & \beta_r(k) > \beta_{max} \\ \beta_{curv}, & \beta_r(k) \in [-\beta_{max}, \beta_{max}] \\ -\beta_{max}, & \beta_r(k) < -\beta_{max} \end{cases} \quad (48)$$

Define the yaw rate $\dot{\psi}_{curv}$ of the desired orientation of autonomous vehicle as

$$\dot{\psi}_{curv} \approx V \cdot C_T / \cos \beta_{curv} \quad (49)$$

For the lateral stability of the vehicle, a constraint of the maximum yaw rate ($\dot{\psi}_{max}$) is defined using the friction coefficient μ, gravity g and the longitudinal velocity V as:

$$\dot{\psi}_{max} = \mu g / V \quad (50)$$

We define the reference signal of yaw rate as

$$\dot{\psi}_r(k) = \begin{cases} \dot{\psi}_{max}, & \dot{\psi}_r(k) > \dot{\psi}_{max} \\ \dot{\psi}_{curv}, & \dot{\psi}_r(k) \in [-\dot{\psi}_{max}, \dot{\psi}_{max}] \\ -\dot{\psi}_{max}, & \dot{\psi}_r(k) < -\dot{\psi}_{max} \end{cases} \quad (51)$$

In the above cases, only for $|\beta(k)| > |\beta_{max}|$, and $|\dot{\psi}(k)| > |\dot{\psi}_{max}|$, the penalties of yaw rate and sideslip angle tracking errors will increase sharply and play a main role in the cost-function.

Suppose that the reference signals $R_r(k)$ from universal potential field and the predicted outputs in $Y_m(k)$ for path tracking are described as:

$$R_r(k) = \begin{bmatrix} X_T(k+1) \\ \beta_T(k+1) \\ \dot{\psi}_T(k+1) \\ \vdots \\ X_T(k+N_p) \\ \beta_T(k+N_p) \\ \dot{\psi}_T(k+N_p) \end{bmatrix}, \quad Y_m(k) = \begin{bmatrix} X_v(k+1) \\ \beta(k+1) \\ \dot{\psi}(k+1) \\ \vdots \\ X_v(k+N_p) \\ \beta(k+N_p) \\ \dot{\psi}(k+N_p) \end{bmatrix} \quad (52)$$

Equation (44) can then be written as:

$$J_E = [R_r(k) - Y_m(k)]^T [R_r(k) - Y_m(k)] + \Delta U_m^T \bar{R} \Delta U_m \quad (53)$$

C. Constraints analysis for MPC

There are three major types of constraints encountered in the path tracking. The first two deal with constraints imposed on the control variables, and the third deals with output constraints.

According to the kinematics and dynamics of vehicle model, the constraints, imposed on steering angle and stability, for path tracking problem are specified as:

$$-C_1 \Delta\delta^{max} \leq \Delta U_m \leq C_1 \Delta\delta^{max} \quad (54)$$

$$-C_1 \delta^{max} \leq C_1 u(k-1) + C_2 \Delta U_m \leq C_1 \delta^{max} \quad (55)$$

$$C_3 \begin{bmatrix} X^{min} \\ -\beta^{max} \\ -\dot{\psi}^{max} \end{bmatrix} \leq F_m X_m(k) + G_m \Delta U_m \leq C_3 \begin{bmatrix} X^{max} \\ \beta^{max} \\ \dot{\psi}^{max} \end{bmatrix} \quad (56)$$

where δ^{max} and $\Delta\delta^{max}$ are the constraints of inputs, X^{max} and X^{min} are the coordinate values of left and right boundaries of road in *X*-direction.

$$C_1 = \begin{bmatrix} 1 \\ 1 \\ \vdots \\ 1 \\ 1 \end{bmatrix}_{Nc \times 1}, \quad C_2 = \begin{bmatrix} 1 & 0 & \cdots & 0 & 0 \\ 1 & 1 & \cdots & 0 & 0 \\ \vdots & \vdots & \ddots & \vdots & \vdots \\ 1 & 1 & \cdots & 1 & 0 \\ 1 & 1 & \cdots & 1 & 1 \end{bmatrix}_{NC \times Nc}$$

$$C_3^T = \begin{bmatrix} 1 & 0 & 0\cdots 1 & 0 & 0 \\ 0 & 1 & 0\cdots 0 & 1 & 0 \\ 0 & 0 & 1\cdots 0 & 0 & 1 \end{bmatrix}_{3N_P \times 3} \quad (57)$$

Subject to the inequality constraints:

$$\begin{bmatrix} M_1 \\ M_2 \\ M_3 \end{bmatrix} \Delta U_m \leq \begin{bmatrix} N_1 \\ N_2 \\ N_3 \end{bmatrix} \quad (58)$$

where the data matrices are:

$$M_1 = \begin{bmatrix} -C_2 \\ C_2 \end{bmatrix}, M_2 = \begin{bmatrix} -I \\ I \end{bmatrix}, M_3 = \begin{bmatrix} -G_m \\ G_m \end{bmatrix}$$
$$N_1 = \begin{bmatrix} C_1\delta^{max} + C_1 u(k-1) \\ C_1\delta^{max} - C_1 u(k-1) \end{bmatrix}, N_2 = \Delta\delta^{max} \begin{bmatrix} C_1 \\ C_1 \end{bmatrix} \quad (59)$$
$$N_3 = \begin{bmatrix} -C_3 \begin{bmatrix} X^{min} \\ -\beta^{max} \\ -\dot{\psi}^{max} \end{bmatrix} + F_m X_m(k) \\ C_3 \begin{bmatrix} X^{max} \\ \beta^{max} \\ \dot{\psi}^{max} \end{bmatrix} - F_m X_m(k) \end{bmatrix}$$

D. Numerous solution using Hildreth's quadratic programming procedure

The next stage is to calculate the future steering inputs that optimize the path-tracking response of the vehicle. We present the following objective function J_E and the constraints by combining equations (41), (53) and (58)

$$J_E = \frac{1}{2}\Delta U_m^T E_m \Delta U_m + \Delta U_m^T F_m \quad (60)$$
$$M_m \Delta U_m \leq N_m \quad (61)$$

where $M_m = [M_1 \quad M_2 \quad M_3]^T$, $N_m = [N_1 \quad N_2 \quad N_3]^T$, E_m, F_m are compatible matrices and vectors in the quadratic programming problem:

$$E_m = 2(G_m^T G_m + \bar{R}) \quad (62)$$
$$F_m = -2{G_m}^T[R_r(k) - F_m X_m(k)] \quad (63)$$

To minimize the objective function subject to inequality constraints, let us consider the following Lagrange expression [29]:

$$J_L = \frac{1}{2}\Delta U_m^T E_m \Delta U_m + \Delta U_m^T F_m + \lambda^T(M_m \Delta U_m - N_m) \quad (64)$$

The dual problem to the original primal problem is derived as:

$$\underset{\lambda \geq 0}{max} \underset{\Delta U_m}{min}(J_L) \quad (65)$$

From the first derivative of the cost function J_L, the minimization over ΔU_m is unconstrained and is attained by:

$$\Delta U_m = -E_m^{-1}(F_m + M_m^T \lambda) \quad (66)$$

Substituting this in (65), the dual problem becomes a quadratic programming problem with λ as the decision variable. The dual problem is written as:

$$\underset{\lambda \geq 0}{min}\left(\frac{1}{2}\lambda^T H_m \lambda + \lambda^T K_m + \frac{1}{2}\lambda^T E_m^{-1}\lambda\right) \quad (67)$$

where matrices H_m and K_m are given by

$$H_m = M_m E_m^{-1} M_m^T \quad (68)$$
$$K_m = N_m + M_m E_m^{-1} F_m \quad (69)$$

Hildreth's quadratic programming procedure was adopted for solving the optimal Lagrange multipliers that minimize the dual objective function [34]. At a given step in the process, we adjust a single component λ_i in vector λ^* to minimize the objective function. The calculation process of λ^* is shown in Fig. 10, and the interested reader is referred to the work of [29] and [35] for details on convergence and implementation. Replacing the decision variable λ in equation (66) with the Lagrange multipliers λ^*, we have:

$$\Delta U_m = -E_m^{-1}(F_m + M_m^T \lambda^*) \quad (70)$$

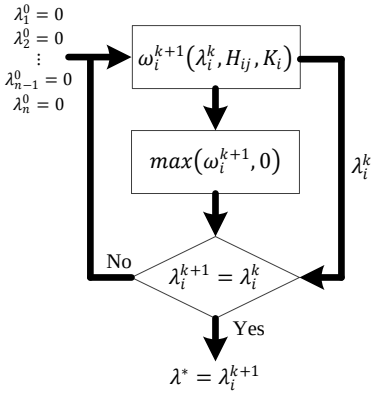

Fig. 10. Hildreth's quadratic programming for MMPC.

VI. Simulations of Path Tracking in Different Scenarios using CarSim and Simulink

To investigate the performance of the proposed framework presented in Section II, numerical simulations with the multi-constrained model predictive controller have been conducted using vehicle simulation software, CarSim, and MATLAB/Simulink. Fig. 11 shows the block diagram of the implementation. In this architecture, a high-fidelity 'big sedan' model in CarSim is used. The MMPC built in the Matlab/Simulink is used to run a closed-loop steering maneuver to track the planned trajectory introduced in Section III. It should be pointed out that the same controller can be used to control the vehicle during different maneuvers.

This set of simulations represents a collision avoidance emergency maneuver in which the vehicle is following the planned trajectory with a given initial forward speed. The control input is the steering angle of front wheels and the goal is to follow the trajectory as close as possible by minimizing the vehicle deviation from the target path. In this context, we assume that future vehicles would be able to identify obstacles on the road such as an animal, rock, or fallen tree/branch, and follow the desired trajectory automatically with a fully autonomous steering system.

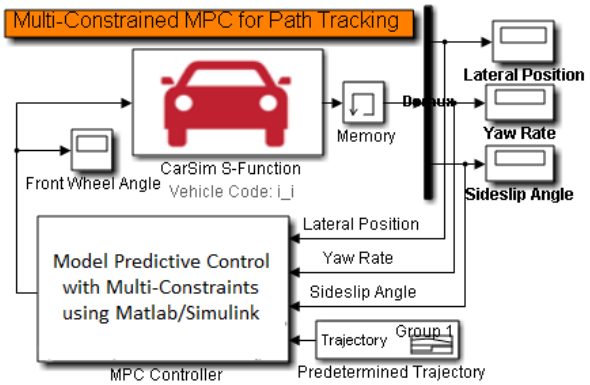

Fig. 11. Architecture of MMPC for path tracking.

Section *A* describes details of the simulation scenario, and Section *B* presents our most important results and findings from simulations.

A. Scenarios description

In the following section, we will refer to a general MPC system with constraint on the front steering angle as controller A, and the proposed MPC system with input constraint on the steering angle of front wheel and state constraints on lateral tracking error, yaw rate, sideslip angle as controller B. The simulation results of controller A are reported and compared with the simulation results of the controller B. The sample time in the simulations of path planning and path tracking are 0.2s and 0.1s respectively.

In the first scenario, suppose a leading vehicle is moving on a straight lane with constant velocity (15m/s, 10m/s, and 0m/s), less than the velocity of the host vehicle (20m/s); this will lead to a collision with the leading vehicle. According to the current position and velocity of the leading vehicle, an alternative trajectory can be generated by the path-planning program on the basis of 3D virtual dangerous potential field, as shown in Fig. 12.

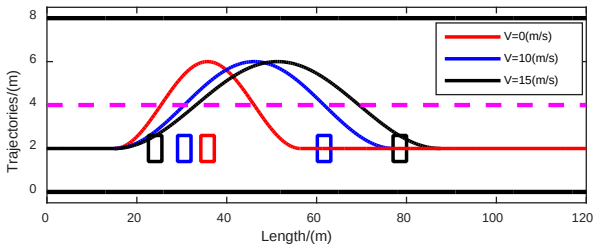

Fig. 12. Planned trajectories for path tracking.

In the second scenario, the initial velocity of the host vehicle is taken as 20 m/s and the leading vehicle is placed at 17.5 m ahead of the host vehicle. Fig. 13(a) shows the predefined acceleration of the leading vehicle, and Fig. 13(b) shows the predefined speed command for the leading vehicle and speed response to the command in the software of CarSim. Applying the above information into the proposed 3D dangerous potential field, a planned trajectory for collision avoidance will be generated as shown in Fig. 13(c).

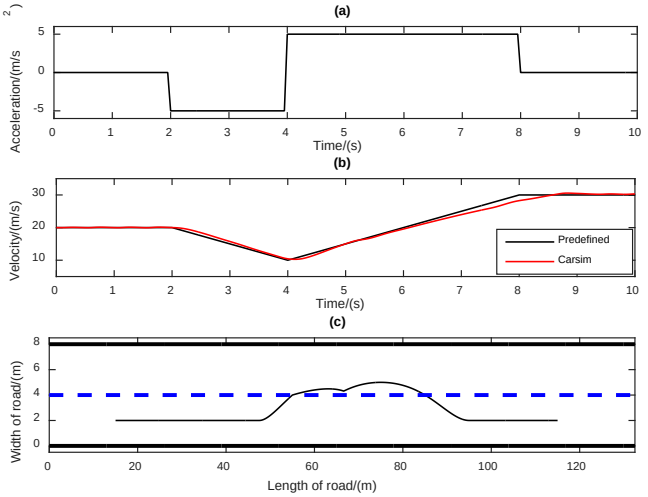

Fig. 13. Predefined information for path tracking. (a) Acceleration of leading vehicle; (b) Velocities of leading vehicle; (3) Planned trajectory derived from 3D potential field for scenario 2.

B. Simulation results

Table I defines the vehicle model parameters.

TABLE I
VEHICLE MODEL PARAMETERS

Symbol	DESCRIPTION	Value[units]
m	Total vehicle mass	2020[kg]
I_z	Yaw moment of inertia	3234[kg · m^2]
V	Velocity of vehicle	20[m/s]
l_f	C.g. distance to front wheels	1.40[m]
l_r	C.g. distance to rear wheels	1.65[m]
C_f	Front wheel cornering stiffness	1420[N/deg]
C_r	Rear wheel cornering stiffness	1420[N/deg]

Scenario 1:

When the leading vehicle is moving at the speed of 10m/s, the host vehicle at a constant velocity of 20 m/s is controlled to track the planned red trajectory in Fig. 12 and is continuously checked to see whether the vehicle will collide with the obstacle.

Fig.s 14 to 16 show the performance comparison, trajectory response, and vehicle response for the designed MPC-based path-tracking controller A and controller B, respectively. Before passing the obstacle (0s$\leqslant$t$\leqslant$2.5s), we observe that both controllers track the paths to avoid the obstacle by turning left. After passing the obstacle (2.5s$\leqslant$t$\leqslant$6s), both controllers bring the vehicle to the centerline of the right lane. In Fig. 14,

controller B exhibits a better path-tracking ability than that of controller A. Controller B, with more constraints than controller A, employs smaller steering input commands and also generates smaller steering angle velocity while controlling the vehicle, as shown in Fig. 15

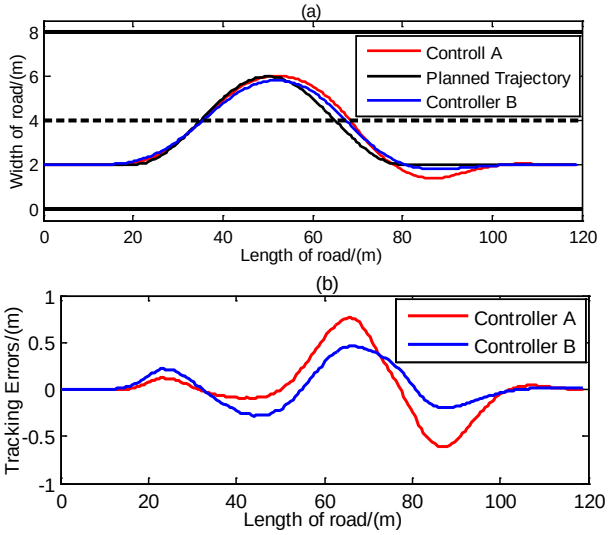

Fig. 14. Simulation results of path tracking. (a) Trajectory tracking; (b) Tracking errors.

The better performance of controller B is also demonstrated by lower levels of yaw rate ($\dot{\psi}$) and sideslip angle of vehicle (β) than those of controller A. In the post-maneuver portion of the test ($t > 2.5s$), controller A is able to steer the vehicle back into the linear region at the maximum steering rate and stabilizes the vehicle, as shown in Fig. 16. Controller B, because of the constraints on the steering angle, steering rate, yaw rate and sideslip angle, always constrains the vehicle within the linear region.

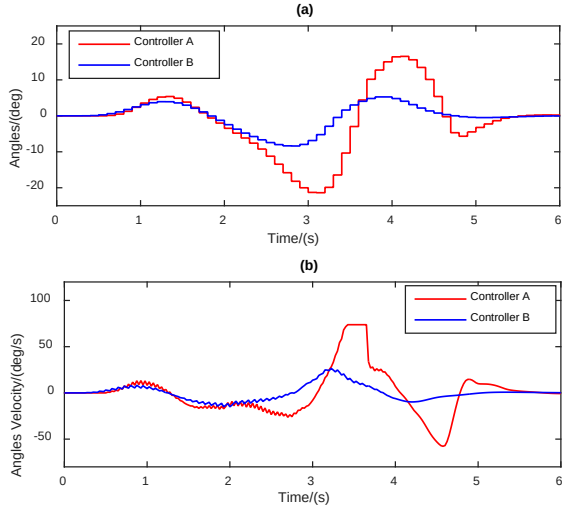

Fig. 15. Control inputs for MMPC. (a) Angles of front wheels; (b) Angles velocity of front wheels.

The simulation results show that both controllers can make the vehicle track the planned trajectory. However, it should be pointed out that a good path-tracking performance with smooth front steering angle, yaw rate, and sideslip angle is obtained using controller B.

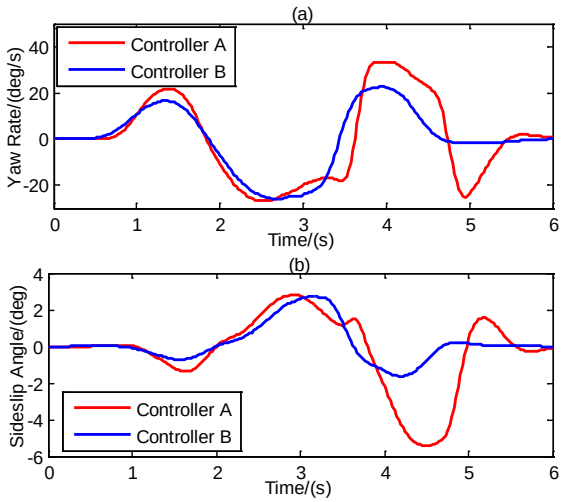

Fig. 16. Stability performance of collision avoidance system. (a) Yaw rates of vehicle; (b) Sideslip angles of vehicle.

Scenario 2:

To evaluate the performance of the path planning program and the MMPC path tracking controller, a moving obstacle with variable velocity as shown in Fig. 13 is considered.

We set μ=0.5 for the friction coefficient in this scenario. Fig. 17 to 19 show the comparison between simulations for the two approaches at 20m/s. Both controllers try to avoid the obstacle by steering to the left, forcing the vehicle to track the planned trajectory. Controller A becomes unstable while controller B avoids the obstacle and is still able to track the planned trajectory.

Fig. 17 shows the trajectories and tracking errors of the vehicle, where the blue and red lines represent the simulation results of controller A and controller B respectively, and the black curve is the planned trajectory computed by the path-planning program.

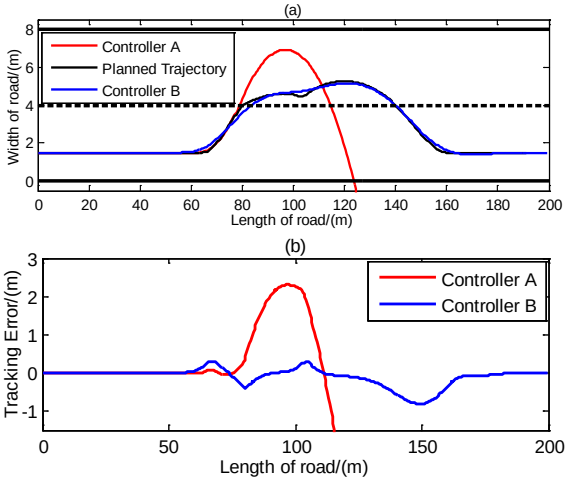

Fig. 17. Tracking performance of MMPC. (a) Planned trajectory and tracking trajectories; (b) Tracking errors.

Controller A is able to keep the vehicle on the planned trajectory at the beginning of collision avoidance. However, once the vehicle deviates too far from the reference, the controller can no longer pull the system back to the planned trajectory and the system becomes uncontrollable. This type of

behavior is induced by tire saturation which results in the sideslip angle and yaw rate of vehicle to exceed the bounds of the stability thresholds [36], as shown in Fig. 19.

We can improve the performance of controller A by extending the prediction horizon $N_p = 20$ and control horizon $N_c = 5$. However, this is done at the expense of computation time, and generates runtime error on the described experimental platform.

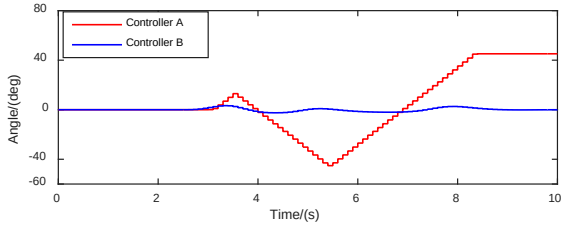

Fig. 18. Angles of front wheels for collision avoidance.

In the post-maneuver portion of the test ($t > 4s$), controller A could not steer the vehicle to track the planned trajectory nor maintain stability even at the maximum steering angle and rate, as shown in Fig. 18. Controller B always constrains the vehicle within the linear region and leads to better tracking performance than Controller A.

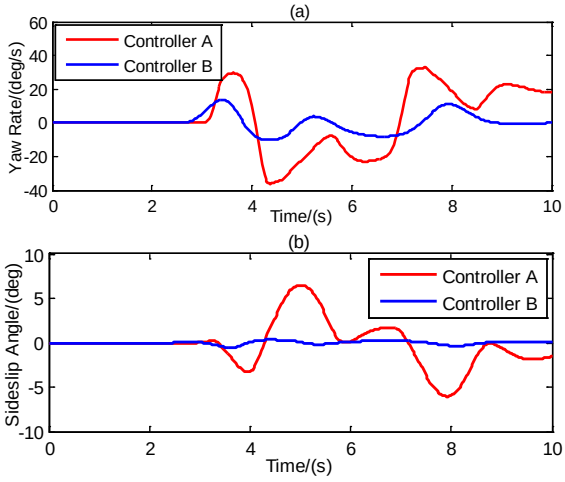

Fig. 19. Stability performance of vehicle. (a) Yaw rate of vehicle; (b) Sideslip angle of vehicle.

VII. Conclusion

In this paper, we presented a framework for path planning and path tracking for a collision avoidance system of autonomous vehicles. The path planning framework built a 3D dangerous potential field based on the information of road and obstacles. A real-time collision free trajectory was then generated for path tracking. As for the path tracking framework, an optimal problem was formulated in terms of cost minimization under constraints in the MMPC method. The state constraints on lateral position, yaw rate, sideslip angle and input constraint on the steering wheel angle were proposed in order to stabilize the vehicle at high speeds. It is solved with Hildreth's quadratic programming procedure and the constraints were incorporated in an augmented vehicle model.

The proposed path tracking framework was implemented and tested in simulations. The MMPC approach was developed in MATLAB/SIMULINK and the actual plant used in the simulations was a CarSim vehicle model. Simulation results demonstrate satisfactory tracking performance in terms of collision avoidance in both static and dynamic environments. The proposed controller was able to stabilize the vehicle on a low friction coefficient road and in the presence of a moving obstacle.

The promising results from the simulations motivated an effort to implement the proposed active safety system. Integration of collision avoidance control with environment information devices such as radar and vision systems are topics of future research.

References

[1] S. Chang, and T. J. Gordon, "A flexible hierarchical model-based control methodology for vehicle active safety systems," *Vehicle Syst Dyn*, vol. 46, pp. 63-75, Sep, 2008.

[2] K. J. Yang, S. K. Gan, and S. Sukkarieh, "An Efficient Path Planning and Control Algorithm for RUAV's in Unknown and Cluttered Environments," *J Intell Robot Syst*, vol. 57, no. 1-4, pp. 101-122, Jan, 2010.

[3] M. P. Aghababa, "3D path planning for underwater vehicles using five evolutionary optimization algorithms avoiding static and energetic obstacles," *Appl Ocean Res*, vol. 38, pp. 48-62, Oct, 2012.

[4] J. Courbon, Y. Mezouar, N. Guenard, and P. Martinet, "Vision-based navigation of unmanned aerial vehicles," *Control Eng Pract*, vol. 18, no. 7, pp. 789-799, Jul, 2010.

[5] S. Saravanakumar, and T. Asokan, "Multipoint potential field method for path planning of autonomous underwater vehicles in 3D space," *Intel Serv Robot*, vol. 6, no. 4, pp. 211-224, Oct, 2013.

[6] V. Kunchev, L. Jain, V. Ivancevic, and A. Finn, "Path planning and obstacle avoidance for autonomous mobile robots: A review," *Lect Notes Artif Int*, vol. 4252, pp. 537-544, 2006.

[7] Y. Kanayama, and B. I. Hartman, "Smooth Local Path Planning for Autonomous Vehicles," *Proceedings - 1989 IEEE International Conference on Robotics And Automation*, Vol 1-3, pp. 1265-1270, 1989.

[8] Z. Shiller, and Y. R. Gwo, "Dynamic Motion Planning Of Autonomous Vehicles," *IEEE T Robotic Autom*, vol. 7, no. 2, pp. 241-249, Apr, 1991.

[9] A. K. Pamosoaji, and K. S. Hong, "A Path-Planning Algorithm Using Vector Potential Functions in Triangular Regions," *IEEE T Syst Man Cy-S*, vol. 43, no. 4, pp. 832-842, Jul, 2013.

[10] A. Shum, K. Morris, and A. Khajepour, "Direction-dependent optimal path planning for autonomous vehicles," *Robot Auton Syst*, vol. 70, pp. 202-214, Aug, 2015.

[11] P. Shi, and Y. W. Zhao, "An Efficient Path Planning Algorithm for Mobile Robot Using Improved Potential Field," *2009 IEEE International Conference on Robotics And Biomimetics (Robio 2009)*, Vols 1-4, pp. 1704-1708, 2009.

[12] T. Shim, G. Adireddy, and H. L. Yuan, "Autonomous vehicle collision avoidance system using path planning and model-predictive-control-based active front steering and wheel torque control," *P I Mech Eng D-J Aut*, vol. 226, no. D6, pp. 767-778, 2012.

[13] F. Rovira-Más, and Q. Zhang, "Fuzzy logic control of an electrohydraulic valve for auto-steering off-road vehicles," *P I Mech Eng D-J Aut*, vol. 222, no. 6, pp. 917-934, Jun, 2008.

[14] S. H. Tabatabaei Oreh, R. Kazemi, and S. Azadi, "A sliding-mode controller for directional control of articulated heavy vehicles," *P I Mech Eng D-J Aut*, vol. 228, no. 3, pp. 245-262, Feb, 2014.

[15] K. Nam, S. Oh, H. Fujimoto, and Y. Hori, "Robust yaw stability control for electric vehicles based on active front steering control through a steer-by-wire system," *Int.J Automot. Technol*, vol. 13, no. 7, pp. 1169-1176, Dec, 2012.

[16] G. V. Raffo, G. K. Gomes, J. E. Normey-Rico, C. R. Kelber, and L. B. Becker, "A Predictive Controller for Autonomous Vehicle Path Tracking," *IEEE T Intell Transp*, vol. 10, no. 1, pp. 92-102, Mar, 2009.

[17] W. Kim, D. Kim, K. Yi, and H. J. Kim, "Development of a path-tracking control system based on model predictive control using infrastructure sensors," *Vehicle Syst Dyn*, vol. 50, no. 6, pp. 1001-1023, Jul, 2012.

[18] M. Hassanzadeh, M. Lidberg, M. Keshavarz, and L. Bjelkeflo, "Path and Speed Control of a Heavy Vehicle for Collision Avoidance Manoeuvres," *2012 IEEE Intelligent Vehicles Symposium (Iv)*, pp. 129-134, 2012.
[19] E. Kim, J. Kim, and M. Sunwoo, "Model predictive control strategy for smooth path tracking of autonomous vehicles with steering actuator dynamics," *Int.J Automot. Technol*, vol. 15, no. 7, pp. 1155-1164, Dec, 2014.
[20] L. Guo, P. S. Ge, M. Yue, and Y. B. Zhao, "Lane Changing Trajectory Planning and Tracking Controller Design for Intelligent Vehicle Running on Curved Road," *Math Probl Eng*, vol.2014, pp. 01-09, Jan, 2014.
[21] D. B. Ren, J. Y. Zhang, J. Zhang, and S. Cui, "Trajectory planning and yaw rate tracking control for lane changing of intelligent vehicle on curved road," *Sci China Technol Sc*, vol. 54, no. 3, pp. 630-642, Mar, 2011.
[22] X. L. Song, H. T. Cao, and J. Huang, "Vehicle path planning in various driving situations based on the elastic band theory for highway collision avoidance," *P I Mech Eng D-J Aut*, vol. 227, no. 12, pp. 1706-1722, Dec, 2013.
[23] M. T. Wolf, and J. W. Burdick, "Artificial potential functions for highway driving with collision avoidance," *2008 IEEE International Conference on Robotics And Automation*, Vols 1-9, pp. 3731-3736, 2008.
[24] H. M. Choset, *Principles of robot motion : theory, algorithms, and implementation*, Cambridge, MA, USA: MIT Press, 2005.
[25] R. Hayashi, J. Isogai, P. Raksincharoensak, and M. Nagai, "Autonomous collision avoidance system by combined control of steering and braking using geometrically optimised vehicular trajectory," *Vehicle Syst Dyn*, vol. 50, pp. 151-168, Jan, 2012.
[26] G. P. Bevan, H. Gollee, and J. O'Reilly, "Trajectory generation for road vehicle obstacle avoidance using convex optimization," *P I Mech Eng D-J Aut*, vol. 224, no. D4, pp. 455-473, 2010.
[27] C. Pozna, F. Troester, R. E. Precup, J. K. Tar, and S. Preitl, "On the design of an obstacle avoiding trajectory: Method and simulation," *Math Comput Simulat*, vol. 79, no. 7, pp. 2211-2226, Mar, 2009.
[28] R. Rajamani, *Vehicle dynamics and control*, New York, NY, USA: Springer, 2012.
[29] L. Wang, *Model predictive control system design and implementation using MATLAB®*, New York, NY, USA: Springer, 2009.
[30] D. J. Cole, A. J. Pick, and A. M. C. Odhams, "Predictive and linear quadratic methods for potential application to modelling driver steering control," *Vehicle Syst Dyn*, vol. 44, no. 3, pp. 259-284, Mar, 2006.
[31] X. X. Na, and D. J. Cole, "Linear quadratic game and non-cooperative predictive methods for potential application to modelling driver-AFS interactive steering control," *Vehicle Syst Dyn*, vol. 51, no. 2, pp. 165-198, Feb 1, 2013.
[32] L. Del Re, F. Allgöwer, L. Glielmo, C. Guardiola, and I. Kolmanovsky, *Automotive model predictive control models, methods and applications*,, New York, NY, USA: Springer, 2010.
[33] U. Kiencke, and L. Nielsen, *Automotive control systems for engine, driveline, and vehicle*, Springer, New York, NY, USA: Springer, 2005.
[34] D. A. Wismer, and R. Chattergy, *Introduction to nonlinear optimization : a problem solving approach*, New York, NY, USA: North-Holland, 1979.
[35] A. N. Iusem, and A. R. Depierro, "On the Convergence Properties Of Hildreth Quadratic-Programming Algorithm," *Math Program*, vol. 47, no. 1, pp. 37-51, May, 1990.
[36] Y. Q. Gao, T. Lin, F. Borrelli, E. Tseng, and D. Hrovat, "Predictive Control Of Autonomous Ground Vehicles with Obstacle Avoidance on Slippery Roads," *Proceedings Of the Asme Dynamic Systems And Control Conference*, Vol 1, pp. 265-272, 2010.

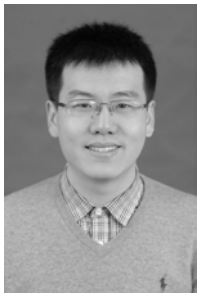

Jie Ji received the B.Sc degree from Chongqing Jiaotong University, Chongqing, China, in 2004, and the Ph.D. degree from Chongqing University, Chongqing, China, in 2010, all in mechanical engineering.

Since July 2010, he has been an Associate Professor with the College of Engineering and Technology, Southwest University, Chongqing, China. From January 2014 to January 2015, he was a Postdoctoral Fellow with the Department of Mechanical and Mechatronics Engineering, University of Waterloo, ON, Canada. His current research interests include vehicle active safety systems, design/analysis of vehicle chassis control systems, intelligent vehicles.

Mr. Ji has been a reviewer for several conferences related to path planning and tracking for intelligent vehicles.

Amir Khajepour received the Ph.D. degree in 1996 from the University of Waterloo, ON, Canada, where he is currently a Professor in the Mechanical and Mechatronics Engineering and the Canada Research Chair in "Mechatronic Vehicle Systems," and serves as the Waterloo Center for Automotive Research Executive Director. He is an expert in systems modeling and control of dynamic systems and has developed an extensive research program that applies his expertise to several key multidisciplinary areas. His research has resulted in several patents, technology transfers, and two start-up companies. He has authored or coauthored more than 350 journal and conference publications, as well as 5 books and 7 book chapters.

Dr. Khajepour is a recipient of the Engineering Medal from Professional Engineers Ontario, is a fellow of the Engineering Institute of Canada, and American and Canadian Society of Mechanical Engineering, and is an Associate Editor of the International Journal of Vehicle Autonomous Systems and International Journal of Powertrain.

Wael William Melek (M'02–SM'06) received the M.A.Sc. and Ph.D. degrees in mechanical engineering from the University of Toronto, Toronto, ON, Canada, in 1998 and 2002, respectively.

Between 2002 and 2004, he was the Artificial Intelligence Division Manager with Alpha Global IT, Inc., Toronto, ON, Canada. He is currently an Assistant Professor with the Department of Mechanical Engineering, University of Waterloo, Waterloo, ON, Canada. His current research interests include mechatronics applications, robotics, industrial automation and the application of fuzzy logic, neural networks, and genetic algorithms for modeling and control of dynamic systems.

Dr. Melek is a member of the American Society of Mechanical Engineers.

Yanjun Huang is currently a PhD student from University of Waterloo, ON, Canada. He received his the M.S. degree in Vehicle engineering from Jilin University, China in 2012. He is working on advanced control strategies and their real-time applications; Heating, Ventilating and Air Conditioning (HVAC) nonlinear dynamic system modeling and control; Modeling of hybrid powertrains, components sizing and power management control strategies design through concurrent optimization and HIL testing.